Archives of Microbiology (2025) 207:109
https://doi.org/10.1007/s00203-025-04316-0

ORIGINAL PAPER

Genome mining reveals the biosynthetic potential of a novel *Lysinibacillus zambalensis* sp. nov., isolated from a hyperalkaline spring

Joyce Amarachi Aja[1] · Lawrence Dave Llorin[1] · Kenji Rowel Q. Lim[2] · Jade Joshua Teodosio[3] · Erwin John Sioson[1,4] · Ron L. Dy[1] · Carlo A. Arcilla[4,5] · Doralyn S. Dalisay[3,6] · Jose Enrico Hizon Lazaro[1]

Received: 21 August 2024 / Revised: 26 February 2025 / Accepted: 22 March 2025 / Published online: 2 April 2025

Abstract

A novel bacterium, designated as strain M3^T, was isolated from a hyperalkaline spring in the Philippines and identified as a new species within the genus *Lysinibacillus* through 16 S rRNA gene sequence and genomic analyses. Although strain M3^T shared a high 16 S rRNA gene sequence similarity (> 98.7%) with many *Lysinibacillus* species, the digital DNA-DNA hybridization and orthologous average nucleotide identity values between strain M3^T and its closet relative, *Lysinibacillus xylanilyticus* DSM 23,493^T, were 41.2% and 90.6%, respectively—both below the established threshold for prokaryotic species delineation. Genome mining of the 5.3 Mbp-draft genome of strain M3^T revealed eight biosynthetic gene clusters, which shared little sequence similarity with characterized clusters, suggesting the potential for encoding novel specialized metabolites. The cells of strain M3^T were Gram-stain-positive, aerobic, rod-shaped, non-motile, and capable of endospore formation. Optimum growth was observed at 30 °C, pH 8.0, and 0.5% (w/v) NaCl. The major respiratory quinone was menaquinone-7, and the predominant polar lipids were diphosphatidylglycerol, phosphatidylethanolamine, phosphatidylglycerol, and two unknown phospholipids. Its fatty acid profile showed an elevated level of iso-$C_{15:0}$, and the peptidoglycan type was determined to be A4α (L-Lys–D-Asp). This study contributes to the growing database and understanding of the genus and aims to help drive future research on the bioactive potential of the genus. *Lysinibacillus zambalensis* sp. nov. is proposed with strain M3^T as the type strain (=TISTR 10640^T=BIOTECH 10973^T).

Keywords *Lysinibacillus* · Hyperalkaline spring · Comparative genomics · Genome mining · Secondary metabolite biosynthetic gene clusters

Communicated by Dmitriy Volokhov.

✉ Jose Enrico Hizon Lazaro
jhlazaro1@up.edu.ph

[1] National Institute of Molecular Biology and Biotechnology, University of the Philippines Diliman, Quezon City, Philippines

[2] Center for Cardiovascular Research, Division of Cardiology, Washington University in St. Louis, St. Louis, MO 63110, USA

[3] Center for Chemical Biology and Biotechnology, University of San Agustin, Iloilo City, Philippines

[4] Philippine Nuclear Research Institute, Quezon City, Philippines

[5] National Institute of Geological Sciences, College of Science, University of the Philippines Diliman, Quezon City, Philippines

[6] Department of Biology, University of San Agustin, Iloilo City, Philippines

Abbreviations

DOC	Dissolved organic carbon
DIC	Dissolved inorganic carbon
LPSN	List of prokaryotic species with standing in nomenclature
dDDH	Digital DNA-DNA hybridization
orthoANI	Orthologous average nucleotide identity
TSA or TSB	Tryptone soya agar or tryptone soya broth
GBDP	Genome BLAST distance phylogeny
UBCG	Up-to-date bacterial core gene set
DPG	Diphosphatidylglycerol
PE	Phosphatidylethanolamine
PG	Phosphatidylglycerol
BGC	Biosynthetic gene cluster
NRPS	Non-ribosomal peptide synthetase
PKS	Polyketide synthase
RiPPs	Ribosomally synthesized and post-translationally modified peptides

Introduction

Alkaline springs may serve as a source of novel bacteria (Baculi et al. 2017). The Poon Bato Spring, Zambales province, Philippines, is situated in ophiolites; the weathering of mineral-rich ultramafic rocks results in waters with high pH of ~11.5 (Baculi et al. 2017; Monnin et al. 2021) and temperatures ranging from 27 to 32 °C (Cardace et al. 2015). The spring exhibited dissolved organic carbon (DOC) concentrations of less than 2 ppm and dissolved inorganic carbon (DIC) concentrations below 20 ppm (Cardace et al. 2015). Baculi et al. (2017) reported that the majority of bacteria isolated from the Poon Bato alkaline spring belonged to the phylum *Bacillota*, with many isolates being capable of producing alkaline enzymes including amylase, protease, lipase, and cellulase.

Members of the genus *Lysinibacillus* are Gram-stain-positive, rod-shaped cells that belong to the family *Bacillaceae* within the phylum *Bacillota*. They were classified as members of the genus *Bacillus* until 2007. Reclassification was based on the discovery that bacteria of the genus *Lysinibacillus* have lysine and aspartic acid in their cell wall peptidoglycan instead of meso-diaminopimelic acid present in *Bacillus* (Ahmed et al. 2007; Nam et al. 2012; Amaresan et al. 2020). The genus *Lysinibacillus* consisted of 22 species with validly published and correct names at the time of writing (Parte 2013, https://lpsn.dsmz.de/genus/lysinibacillus), with *Lysinibacillus boronitolerans* T-10a^T as the type strain (Ahmed et al. 2007). *Lysinibacillus* species are ubiquitous in soil (Ahmed et al. 2007) and have been isolated from diverse environments including deep-sea sediments (Yu et al. 2019), and even pufferfish liver (Wang et al. 2010). *Lysinibacillus* species have also been isolated from alkaline-fermented leaves (Ouoba et al. 2015), saline-alkaline soils (Kong et al. 2014; Sun et al. 2017), and the alkaline Lonar Lake water in India (Tambekar et al. 2016).

Members of the genus may serve as a source of pharmacologically relevant compounds (Jamal and Ahmad 2022). *Lysinibacillus* spp. produce a variety of bacteriocins that are effective against foodborne bacterial and fungal pathogens (Ahmad et al. 2014; Ahmad and Khan 2015). Bacteriocins, ribosomally synthesized peptides that are often post-translationally modified, can kill or inhibit other bacterial strains but will not harm the producing strain (Yang et al. 2014; Dicks et al. 2018). A novel bacteriocin, produced by *Lysinibacillus* sp. strain JX416855, showed broad-spectrum antibacterial activity and strongly inhibited the fungi *Aspergillus*, *Fusarium*, and *Trichoderma* (Ahmad et al. 2014). *L. sphaericus* ZA9 produces 2-penthyl-4-quinolinecarboxylic acid, an antifungal compound, as well as binary toxin Cry48/Cry49 which possesses antimalarial and larvicidal properties (Naureen et al. 2017). *L. odysseyi* KC149512 produces compounds with antimicrobial, anticancer, antioxidant, and anti-inflammatory properties (Karthick and Mohanraju 2020). *L.* sp. AS-1 (Maela et al. 2022), L. sp. MK212927 (El-Sayed et al. 2022)d *fusiformis* S9 also produces bioactive compounds (Pradhan et al. 2014).

Despite the potential of numerous bacterial species to produce new bioactive compounds, genetically encoded secondary metabolites (SMs) often escape detection by conventional approaches (Monciardini et al. 2014). These constraints may be overcome by mining the genome for biosynthetic gene clusters (BGCs), including transcriptionally silent BGCs (Kalkreuter et al. 2020). Bioinformatic algorithms identify signatures from genomic information and help to prioritize strains or BGCs for investigation, potentially making the discovery of new compounds more efficient (Albarano et al. 2020; Kalkreuter et al. 2020). Using this approach, a previously uncharacterized bacteriocin gene cluster in *L. boronitolerans* was identified via genome sequencing and bioinformatic analysis, which led to its characterization via heterologous expression in *Escherichia coli*. The product of the BGC inhibited the growth of several pathogenic bacteria (Tang et al. 2023). In addition, genome mining and prioritizing of an orphan polyketide synthase-nonribosomal synthase (PKS-NRPS) hybrid gene cluster from the genus *Salinispora* led to the identification of thiotetronic acid natural products via heterologous expression (Tang et al. 2015). Chemical synthesis can be used to synthesize predicted compounds known as synthetic-bioinformatic natural products (syn-BNPs). The syn-BNPs may have only a resemblance to the original natural products because the post-assembly modifications of the original compound may not be accurately predicted (Scherlach and Hertweek 2021). A syn-BNP, humimycin A, which has high efficacy against methicillin-resistant *Staphylococcus aureus* (MRSA), was identified via chemical synthesis of an NRPS gene cluster from *Rhodococcus equi* (Chu et al. 2016).

This study describes the genomic, phenotypic, and chemotaxonomic analyses of strain M3^T, isolated from the Poon Bato Spring in Botolan, Zambales, Philippines. Genome mining revealed a diverse array of BGC classes, including siderophores, polyketide synthases, nonribosomal peptide synthases, ribosomally synthesized and post-translationally modified peptides (RiPPs), opine-like metallophores, and betalactones, with low sequence similarities to experimentally characterized BGCs in the Minimum Information about a Biosynthetic Gene cluster (MIBiG) database. This unique genomic, phenotypic, and chemotaxonomic profile suggests that strain M3^T represents a previously uncharacterized species with potentially novel biochemical and bioactive properties. We propose to assign strain M3^T to a new species, *Lysinibacillus zambalensis* sp. nov.

Materials and methods

Strain isolation

Strain M3^T was isolated from water samples collected from the Poon Bato, Zambales hyperalkaline spring in the Philippines (latitude 15.32214° N, longitude 120.07404° E). Samples were diluted and plated on tryptone soya agar (TSA) plates (pH 8.5), and incubated at 30 ˚C for 24 to 72 h. The culture medium was obtained from TM Media (Delhi, India), a manufacturer of microbiological media. Isolates that grew well in pH 8.5 media were selected and subcultured repeatedly to obtain pure cultures. The pure cultures were stored at -80 °C in 50% glycerol prepared by mixing equal volumes of glycerol and bacterial broth culture (TSB, pH 8.5) and used for 16 S rRNA identification and further physiological and biochemical characterization.

Whole genome sequencing, assembly, and annotation

Genomic DNA was extracted using the Qiagen QIAamp DNA Mini Kit according to the manufacturer's instructions. Routine quality checks were performed via Qubit and TapeStation220. Library preparation was performed using the TruSeq DNA Nano Library Preparation Kit. DNA sequencing was performed using the NextSeq 500/550 High Output Kit (2 × 150 cycles) on the Illumina NextSeq™ 500 Sequencing system.

The online bioinformatics platform Bacterial Genome Assembly Service of the Bacterial and Viral Bioinformatics Resource Center (BV-BRC; https://www.bv-brc.org/; Olson et al. 2023) was used to trim and assemble raw sequencing read data. The sequences were trimmed via TrimGalore (v0.6.5, www.bioinformatics.babraham.ac.uk/projects/trim_galore/), and SPAdes v4.0.0 (Bankevich et al. 2012) was used for *de novo* assembly. The genome was annotated using both the BV-BRC platform with *Lysinibacillus xylanilyticus* DSM 23,493^T as the reference strain, and the Rapid Annotations using Subsystems Technology (RAST) version 2 RASTtk pipeline (Aziz et al. 2008; Overbeek et al. 2014; Brettin et al. 2015). BUSCO version 5.6.1 was used to assess the completeness of the genome assembly (Manni et al. 2021). The BV-BRC algorithm, which employs EvalG, was also used to analyze the genome quality (Olson et al. 2023). EvalG implements the CheckM algorithm (Parks et al. 2015) to assess the genome's completeness and contamination.

Phylogenetic analysis based on 16 S rRNA gene and whole genome

The 16 S rRNA gene of strain M3^T was amplified by PCR with the universal 27F and 1492R primers as well as the 518 F and 800R primers (Senthilraj et al. 2016). The amplicons were sequenced using Sanger dideoxy sequencing at Macrogen, Korea. The contigs were assembled using CAP3 (Huang and Madan 1999). The sequences were assembled to generate the nearly complete 16 S rRNA gene sequence (1407 nucleotides) of strain M3^T (GenBank accession number PQ061501). Additionally, the 16 S rRNA gene sequences of strain M3^T and related *Lysinibacillus* species were extracted from the genome using the ContEst16S algorithm (Lee et al. 2017) available in the EzBioCloud server (Chalita et al. 2024). The 16 S rRNA gene sequences of *L. mangiferihumi* M-GX18^T (JF731238), *L. parviboronicapiens* BAM-582^T (AB333000598), *L. fusiformis* ATCC 7055^T (AJ310083), *L. odysseyi* 34hs-1^T (AF526913), and *L. alkalisoli* CGMCC 1.15760^T (MT759970), on the other hand, were retrieved from the accession numbers listed in the LPSN database (Parte 2013, https://lpsn.dsmz.de/genus/lysinibacillus) due to the inability to extract their respective 16 S rRNA gene sequences using the ContEst16S algorithm. The 16 S rRNA gene sequence of strain M3^T and other *Lysinibacillus* species were aligned using the ClustalW algorithm (Thompson et al. 1994) in MEGA 11 (Tamura et al. 2021). Phylogenetic trees were constructed using the maximum-likelihood (Felsenstein 1981), neighbor-joining (Saitou and Nei 1987), and maximum parsimony algorithms (Fitch 1971), with bootstrap analysis based on 1,000 replications (Felsenstein 1985); *Bacillus subtilis* DSM 10^T was used as the outgroup. The percent identities of strain M3^T compared to related type strains were determined using the NCBI BLAST algorithm (Altschul et al. 1997) (Table S1).

Phylogenomic analysis of strain M3^T based on the whole genome sequence was carried out as described by Alam et al. (2022). Briefly, the assembled genome of strain M3^T and related *Lysinibacillus* species from the LPSN database (Parte 2013) were run through the Type (Strain) Genome Server (TYGS) (available at https://tygs.dsmz.de/; Meier-Kolthoff and Göker 2019). The phylogenomic tree was inferred using FastME2.1.6.1 (Lefort et al. 2015) from Genome BLAST distance phylogeny (GBDP) distances calculated from the genomic sequences. The branch lengths were scaled in terms of GBDP formula d_5. The trees were rooted at the outgroup. Additionally, the phylogenomic tree based on 81 core genes of strain M3^T and related strains was constructed with the UBCG (Up-to-date bacterial core gene set) version 3.0 pipeline (Na et al. 2018).

The digital DNA-DNA hybridization (dDDH) values were calculated using the Genome-to-Genome Distance

Calculator (GGDC) v3.0 (Meier-Kolthoff et al. 2022) using the recommended formula 2 (identities / length of high-scoring segment pairs), and the corresponding heatmap was generated using MORPHEUS (https://software.broadinstitute.org/morpheus). The orthologous average nucleotide identity (orthoANI) values and the corresponding heatmap were generated using the OAT software v0.93.1 (Lee et al. 2016). The genome characteristics, 16 S rRNA gene percent similarity to strain M3^T, size, G+C content, and accession numbers) of the *Lysinibacillus* species used in this study are found in Table S1.

Gram Staining, *Endospore Staining*, *and Scanning Electron Microscopy*.

Gram staining was carried out according to standard procedure (Froböse et al. 2020). Endospore staining was carried out on an 18–24 h-old TSB culture of strain M3^T with the Schaeffer-Fulton method, using malachite green and safranin as dyes (Schaeffer and Fulton 1933). For scanning electron microscopy, a colony of strain M3^T was fixed using 2.5% glutaraldehyde and incubated at 4 °C for 4 h. The fixed bacterial suspension was washed with phosphate-buffered saline (PBS). Then, the bacterial pellets were resuspended in 1 mL of 1% PBS to remove the insoluble salts. A 5 µL aliquot of the bacterial suspension was mounted onto a copper tape and allowed to air dry overnight. The dried suspension was sequentially dehydrated for approximately 10 min each with 20%, 40%, 60%, 80%, and 100% ethanol. The specimen was placed in an aluminum stub (JEOL Ø25 × 10 mm cylinder SEM sample stub TM, Tokyo, Japan), followed by sputter coating with gold for 30 s using the JEOL Smart Coater TM (Tokyo, Japan) to enhance sample conductivity. The morphology of the cells was observed using the JCM-7000 NeoScope™ Benchtop SEM (Tokyo, Japan) in high vacuum mode.

Phenotypic characterization

The optimum growth conditions of strain M3^T were determined by growing the bacterium in TSB at temperatures ranging from 5 ˚C to 45 ˚C (5, 15, 25, 30, 37, 45) and pH ranging from 4 to 12 (4, 5, 6, 7, 8, 9, 10, 11, 12). A seed culture was prepared by inoculating a single colony of strain M3^T into 5 mL of TSB at 37 ˚C overnight. The seed culture was then used to inoculate 100 mL of TSB and the broth cultures were incubated at the different temperatures for 7–8 h. To test for pH tolerance, 1 mL of a strain M3^T seed culture was used to inoculate 100 mL of TSB which was adjusted to pH values ranging from 4 to 12. The pH of the media was adjusted using acetate buffer for pH 4 to 6, glycine-NaOH buffer for pH 9 to 12, and HCl or NaOH for pH 7 and 8. The final pH of each medium was verified using a pH meter before inoculation. NaCl tolerance was determined by inoculating 500 µL of the seed culture in 150 mL of TSB with NaCl at concentrations ranging from 0.5 to 18% (0.5, 3, 6, 9, 12, 15, 18). The cultures for the pH and NaCl tolerance tests were incubated at 30 ˚C for 7–8 h under aerobic conditions. The optical densities (OD) were measured at 600 nm using a NanoDrop™ 2000c spectrophotometer. The OD_{600} was measured to monitor cell growth. For antibiotic sensitivity testing, antibiotic-impregnated filter paper discs (ciprofloxacin and penicillin G) were placed on Muller-Hinton Agar plates inoculated with a strain M3^T culture, which was evenly spread on the agar surface using a sterile swab. The plates were then incubated at 35 °C for 24 h to assess bacterial growth inhibition (Mounyr et al. 2016).

Cell growth under anaerobic conditions was determined by culturing strain M3^T under a layer of sterile mineral oil (Umehara and Aoyagi 2023). The BIOLOG GEN III Microplate analysis of strain M3^T was carried out according to the standard protocol (Ngalimat et al. 2019). This assay comprised 94 tests: 71 for carbon source utilization and 23 for chemical sensitivity. Motility was assessed by inoculating a soft TSA medium (0.4% agar) with strain M3^T, followed by incubation for 7 days. Catalase activity was determined by adding 3% hydrogen peroxide to a single colony and observing bubble formation while oxidase activity was tested using 1% (v/v) tetramethyl p-phenylenediamine, with a color change indicating a positive result (Reiner 2010; Shields and Cathcart 2010). To test for nitrate reduction, sulfanilic acid and α-naphthylamine reagents were added to nitrate broth (Buxton 2011). Methyl Red and Voges-Proskauer (VP) tests were performed by adding methyl red (MR) reagent and α-naphthol/KOH, respectively, to MR-VP broth, according to McDevitt (2009). Lysine decarboxylase activity was evaluated using Moeller's lysine decarboxylase agar (Lal and Cheeptham 2015) while the ability of strain M3^T to use citrate as a carbon source was determined using Simmons citrate agar slants (MacWilliams 2009a, b). Urease activity was tested by inoculating urea broth and observing a color change from yellow to pink (Brink 2010), and indole production was detected by adding Kovac's reagent to tryptone broth (MacWilliams 2009a, b).

Chemotaxonomic analysis

Analyses of cellular fatty acids, respiratory quinones, polar lipids, whole-cell sugars, and the peptidoglycan structure of strain M3^T were carried out by DSMZ Services, Leibniz-Institut DSMZ – Deutsche Sammlung von Mikroorganismen und Zellkulturen GmbH, Braunschweig, Germany. Briefly, the cellular fatty acids were evaluated using the Microbial Identification System (MIDI; microbial ID) protocols. Respiratory quinones were extracted with hexane from freeze-dried cell material and purified by silica-based

solid-phase extraction, followed by analysis by HPLC analysis using a reverse phase column and recording absorption spectra (Vieira et al. 2021). Polar lipids were analyzed using a modified protocol by Bligh and Dyer (1959). Polar lipids were extracted from freeze-dried cells using chloroform: methanol:0.3% aqueous NaCl mixture and separated by two-dimensional silica gel thin layer chromatography (TLC). TLC on cellulose plates was used to determine the diagnostic sugars in whole-cell hydrolysates of strain M3^T. Peptidoglycans were analyzed according to the protocol described by Schumann (2011). The identity of all amino acids was confirmed by agreement in the gas-chromatographic retention time with those of the standards and by characteristic mass spectrometric fragment ions of the derivatives.

Identification of Putative Biosynthetic Gene Clusters (BGCs).

Putative secondary metabolite BGCs were predicted using antiSMASH v7.0 (Blin et al. 2023). For antiSMASH, the detection strictness was set to "relaxed", and all the extra features were selected: KnownClusterBlast, ClusterBlast, SubClusterBlast, MIBiG cluster comparison, ActiveSiteFinder, RREFinder, Cluster Pfam analysis, Pfam-based GO term annotation, and TIGRFam analysis. BAGEL4 was used to mine the genome for RiPPS and bacteriocins (van Heel et al. 2018). RiPPMiner was used for sequence comparison of RiPPs (Agrawal et al. 2017).

Results and discussion

Genomic and phylogenetic analyses

The draft genome of strain M3^T had a size of 5,298,580 bp (~5.3 Mbp) within 129 contigs; the mean DNA G+C content was 36.5%. The draft genome consisted of 5,175 coding sequences, 16 rRNAs, and 73 tRNAs (Table S2). The draft genome of strain M3^T has been deposited in the GenBank database under the accession number JBEGDG000000000. The BV-BRC algorithm determined that the completeness and contamination scores of the draft genome were 99.9% and 1.9%, respectively (Table S2), while BUSCO analysis indicated a completeness score of 99.1% (data not shown). According to the RAST annotation, 322 subsystems were identified with the majority of the genes being associated with amino acid and derivative metabolism and carbohydrate metabolism (Fig. S1). No plasmid DNA was detected in the genome, according to the BV-BRC and RAST annotations.

Strain M3^T shared high 16 S rRNA gene sequence similarity (>98.7%) with several *Lysinibacillus* species, having the highest similarity (99.7%) with the type strain *L. xylanilyticus* DSM 23,493^T (Table S1). In the maximum likelihood and maximum parsimony phylogenetic trees, strain M3^T formed a monophyletic lineage with *L. xylanilyticus* DSM 23,493^T, and their closest relative was "*L. agricola*" FJAT-51,161^T (Fig. 1 and Fig. S2). However, in the phylogenetic tree analyzed using the neighbor-joining algorithm, strain M3^T formed a monophyletic lineage with "*L. agricola*" FJAT-51,161^T, and their closest relative was *L. xylanilyticus* DSM 23,493^T (Fig. S2). Although listed as a child taxon in the LPSN database, the name "*L. agricola*" has not been validly published (Parte 2013).

Several studies indicated that species with high 16 S rRNA gene sequence similarity may still be classified as distinct (Stackebrandt and Goebel 1994). For example, the *Bacillus subtilis* group comprises eight closely related species that cannot be differentiated by 16 S rRNA gene sequence analysis, exhibiting similarities of 98.1-99.8% (Wang et al. 2007). This applies to other genera, including *Mycobacterium* (Blackwood et al. 2000) and *Streptomyces* (Komaki 2023). This issue highlights the potential challenges with 16 S rRNA gene-based classification, particularly in the misclassification of novel species.

To further confirm species delineation of strain M3^T, digital DNA-DNA hybridization (dDDH) and orthologous average nucleotide identity (orthoANI) values were calculated. In contrast to 16 S rRNA gene similarities, dDDH and ANI analyses provide a comprehensive evaluation of genetic relatedness and allow for more accurate species distinctions (Goris et al. 2007). Strain M3^T and its closest relative, *L. xylanilyticus* DSM 23,493^T, showed dDDH and orthoANI values of 41.2% and 90.6%. respectively (Fig. 2A and B). The dDDH and orthoANI values of strain M3^T and "*L. agricola*" FJAT-51,161^T were 40.1% and 89.8%, respectively. The recognized cutoff values for prokaryotic species delineation are 70% for dDDH and 95% for ANI (Goris et al. 2007), suggesting strain M3^T represents a novel species within the genus *Lysinibacillus*.

The phylogenomic tree based on whole genome sequences further confirmed the close relationship between strain M3^T and *L. xylanilyticus* DSM 23,493^T (Fig. 3A). This topology was consistent with the phylogenomic tree based on the concatenation of 81 core genes in strain M3^T and several *Lysinibacillus* species (Fig. 3B).

Phenotypic characterization of strain M3^T

The colonies of strain M3^T appeared round, creamy white, with an entire margin, slightly raised elevation, and an opaque appearance on tryptone soya agar (TSA) after 18 h of incubation (Fig. S3A). The cells were found to be Gram-stain-positive and formed ellipsoidal, terminal endospores (Fig. S3B). Strain M3^T grew within a temperature range of 25–37 °C, with optimum growth at 30 °C (Fig. S4A). It

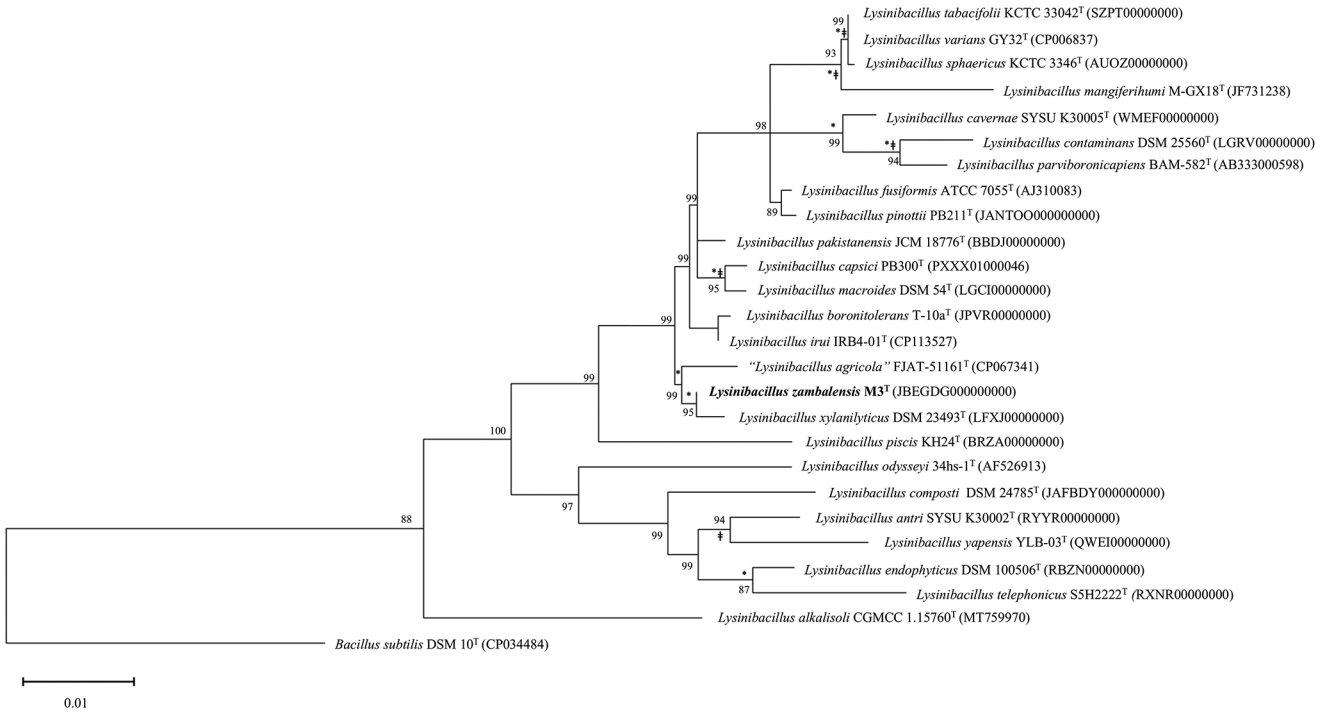

Fig. 1 Maximum-likelihood phylogenetic tree based on the 16 S rRNA gene sequence of strain M3^T and closely related *Lysinibacillus* species. Bootstrap values are expressed as percentages of 1000 replications. The GenBank accession numbers of the genomes, from which the 16 S rRNA gene sequences were extracted using the ContEst16S algorithm on the EzBioCloud server, or the accession numbers of the 16 S rRNA gene sequences, are specified in parentheses. Names not validly published are indicated in quotation marks. Asterisks and crosses denote branches identified through the maximum parsimony and neighbor-joining methods, respectively

demonstrated a pH tolerance at a range of 6–10, with optimum growth at pH 8 (Fig. S4B). Growth at pH 10 suggests its tolerance for alkaline conditions. Strain M3^T exhibited growth in media containing 0.5–3% NaCl, with optimal growth at 0.5% (Fig. S4C). The growth characteristics of strain M3^T were slightly different compared to its closest relatives with *L. xylanilyticus* DSM 23,493^T growing in pH 5–9 and "*L. agricola*" FJAT-51,161^T growing in pH 7–9 (Table 1). Like strain M3^T, strains *L. xylanilyticus* DSM 23,493^T and "*L. agricola*" FJAT-51,161^T grow optimally at 30 °C (Lu and Liu 2021).

Scanning electron microscopy revealed a rod-shaped cellular structure measuring up to 3 µm in length and 0.6 µm in width, with flagella-like structures (Fig. 4). The presence of flagella-like structures is further supported by the identification of 43 flagella-related genes in the RAST annotation (Fig. S1). However, agar motility assays demonstrated that strain M3^T was non-motile. While many species of *Lysinibacillus* are motile, *L. fusiformis* has been reported as non-motile (Ahmed et al. 2007). The flagella-like structures observed in strain M3^T may be influenced by regulatory or environmental factors affecting flagellar gene expression, as seen in enteroinvasive *Escherichia coli* (EIEC) strains, which are typically non-motile but can produce functional flagella under specific conditions (Andrade et al. 2002). Additionally, flagella may have functions other than motility, including secretion, adhesion, and biofilm formation (Chaban et al. 2015; Akahoshi and Bevins 2022). Future studies are needed to elucidate the role and regulation of flagella in strain M3^T.

Strain M3^T exhibited no growth under anaerobic conditions. Biochemical analysis of strain M3^T showed that it was catalase positive, lysine decarboxylase positive, citrate negative, indole negative, methyl red negative, nitrate reduction negative, oxidase negative, urease negative, and Voges-Proskauer negative. It displayed susceptibility (inhibition zone diameter greater than 25 mm) to ciprofloxacin (5 µg/disc) and penicillin G (10 µg/disc). Analysis for carbon utilization and chemical sensitivity using the BIOLOG GEN III Microbial Identification system showed that strain M3^T did not match with any known species' profile in the BIOLOG database; it shared low similarity scores of 0.455 and 0.115 with the closest reference organisms *Bacillus decisifrondis* and *L. boronitolerans*, respectively (Table S3). *B. decisifrondis* was identified in 2007 (Zhang et al. 2007)—the same year that a new taxonomic classification parameter split *Lysinibacillus* species from the *Bacillus* genus (Ahmed et al. 2007). It has since been reclassified as *Lysinibacillus* sp. FJAT-14,222 according to the data from the NCBI BioProject accession number PRJNA294250 (https://www.ncbi

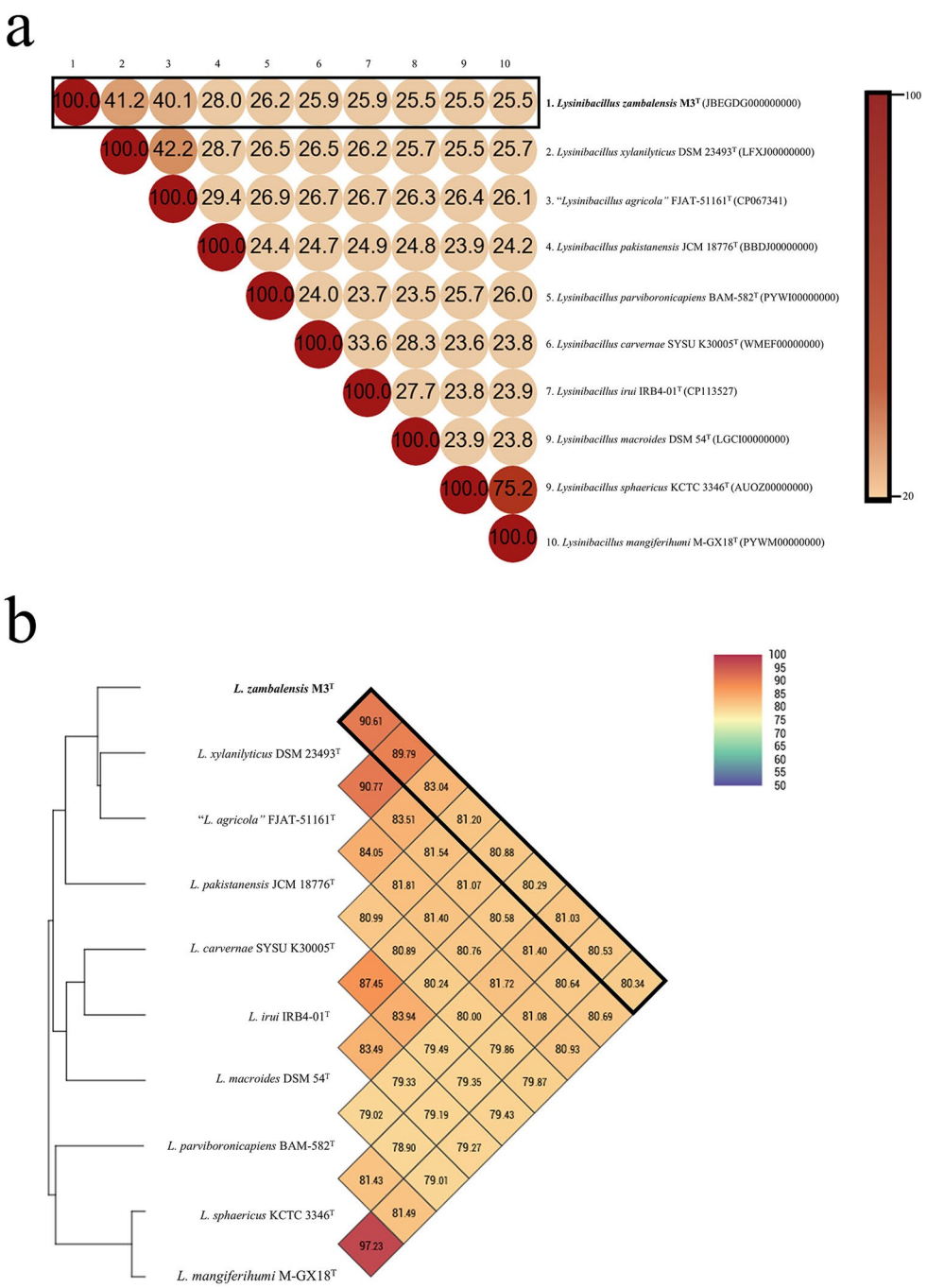

Fig. 2 Pairwise comparisons of (**A**) digital DNA-DNA hybridization (dDDH) and (**B**) orthologous average nucleotide (orthoANI) values between strain M3^T and its closely related type strains. Values in the dark box show the comparisons between strain M3^T and related type strains. The color bar indicates the similarity between the compared strains, ranging from (**A**) light orange to red or from (**B**) blue to red. As the color intensity transitions towards red, it indicates a closer relationship between the strains. Names not validly published are indicated in quotation marks

.nlm.nih.gov/bioproject/?term=PRJNA294250). *Lysinibacillus* sp. FJAT-14,222 clustered with *Lysinibacillus* species in phylogenomic analyses (Fig. 3).

In the BIOLOG assay, strain M3^T exhibited the ability to utilize D-gentibiose, D-turanose, glycerol, L-fucose, and N-acetyl-D-glucosamine, similar to its closest relative *L. xylanilyticus* DSM 23,493^T (Lee et al. 2010). However, strain M3^T could be differentiated from *L. xylanilyticus* DSM 23,493^T by its inability to utilize maltose, sucrose, rhamnose, and sorbitol (Table 1). Additional distinct characteristics of strain M3^T in relation to its close phylogenetic neighbors are displayed in Table 1.

Chemotaxonomic analysis

Chemotaxonomic analysis examines macromolecule distribution to assess the relatedness of bacterial strains to known species (Gokdemir and Aras 2019). The chemotaxonomic characteristics of strain M3^T were compared to those of *L. xylanilyticus* DSM 23,493^T, *"L. agricola"* FJAT-51,161^T, *L. macroides* DSM 54^T, and *L. boronitolerans* T-10a^T

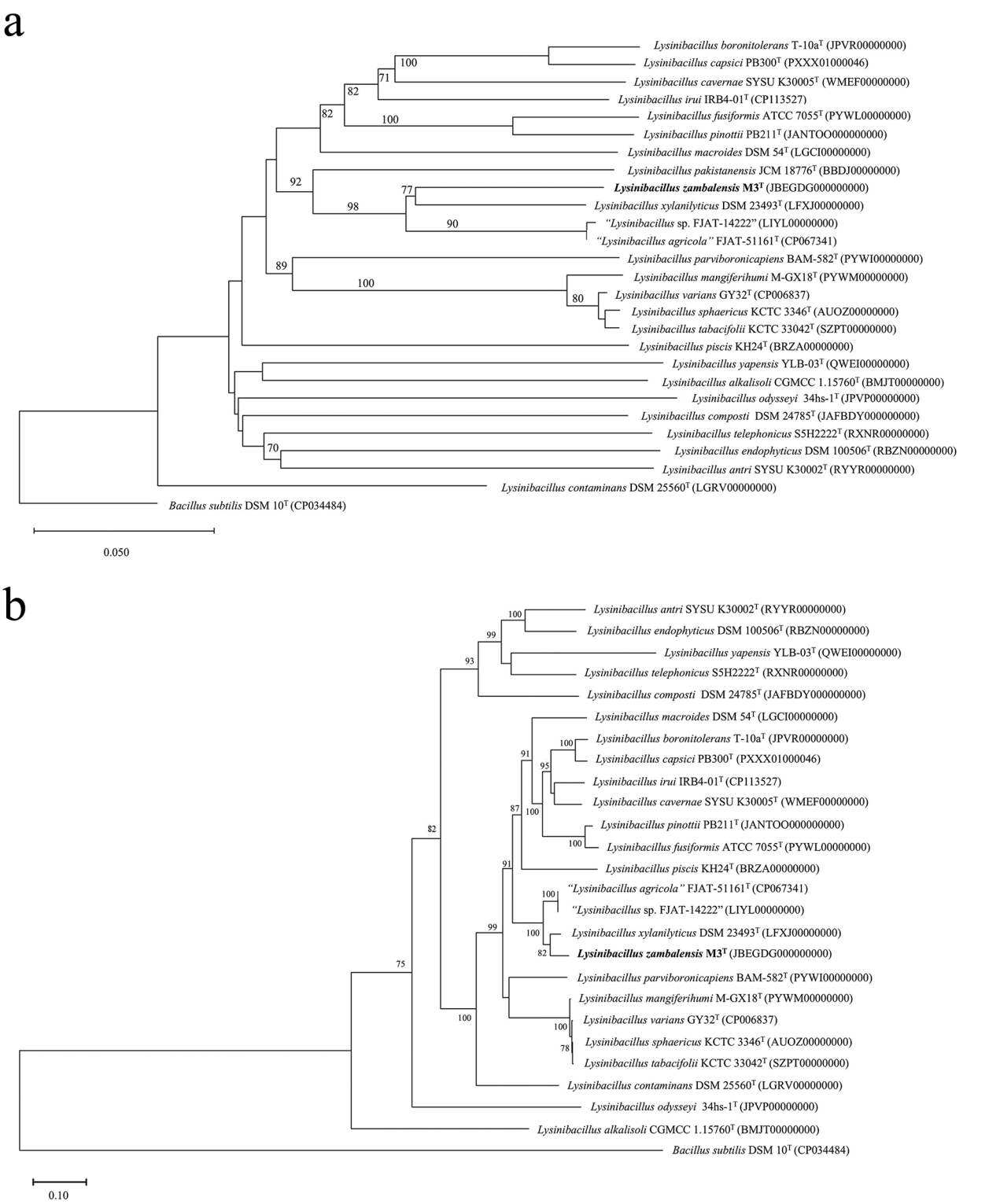

Fig. 3 (**A**) GBDP phylogenomic tree of strain M3^T compared to closest relatives based on whole genome sequences and (**B**) phylogenomic tree based on 81 aligned UBCG sequences of strain M3^T and related *Lysinibacillus* species. Bootstrap values are given at the nodes; only values above 70% are indicated. *Bacillus subtilis* DSM 10^T was used as the outgroup species. Names not validly published are indicated in quotation marks

Table 1 Comparative features of strain M3^T and its closely related species

Characteristics	1	2 [a]	3 [b]	4 [c]	5 [d]
Cell size (μm)	0.6 × 3.0	0.8–1.0 × 3.0–5.0	0.8-1.1 × 2.0-3.4	0.9-1.1 × 3.0-5.0	0.8-1.5 × 3.0-5.0
Spore shape	R/O, T	R, T	R, T	R/O, T	R/O, T
Motility	Non-motile	Motile	Motile	Motile	Motile
pH range	6–10	5–9	7–9	7–9	5.5–9.5
pH optimal	7	NA	7	8	7
Temp range (°C)	15–45	10–45	25–40	10–45	16–45
Temp optimal (°C)	30	30	30	30	37
Oxidase	-	+	+	-	+
Indole	-	-	NA	-	-
Urease	-	NA	-	-	+
Voges-Proskauer	-	-	+	+	+
Hydrolysis of gelatin	+/w	+	+	+/w	-
Arginine dihydrolase	-	-	-	-	+
Lysine decarboxylase	+	-	+	-	-
Utilization of: *					
Citrate	-	+	NA	-	+
Maltose	-	+	NA	NA	-
Trehalose	-	-	NA	NA	-
Sucrose	-	+	NA	NA	-
Melibiose	+/w	+	NA	NA	-
Mannose	-	-	NA	NA	-
Rhamnose	-	+	NA	NA	-
Sorbitol	-	+	NA	NA	-

1, Strain M3^T; 2, *L. xylanilyticus* DSM 23,493^T; 3, "*L. agricola*" FJAT-51,161^T; 4, *L. macroides* DSM 54^T; 5, *L. boronitolerans* T-10a^T. All strains are Gram-stain-positive and endospore forming. All strains are catalase positive and negative for nitrate reduction. Strain M3^T and related strains exhibit differences in motility, oxidase activity, lysine decarboxylation, and the utilization of various carbon sources including citrate, maltose, sucrose, melibiose, rhamnose, and sorbitol. All data was from this study unless indicated otherwise. O, oval or slightly oval; R, round; T, terminal; +, positive; -, negative; +/w, weakly positive; NA, no data available

[a] Data from Lee et al. (2010), [b] Data from Lu and Liu (2021), [c] Data from Coorevits et al. (2012), [d] Data from Ahmed et al. (2007), * Data were taken from Lee et al. (2010) for the reference species *L. xylanilyticus* DSM 23,493^T and *L. boronitolerans* T-10a^T

(Table 2). The two respiratory quinones of strain M3^T were MK-7 (94.2%) and MK-6 (5.8%), with MK-7 having the highest percentage, a characteristic shared by many species of *Lysinibacillus*. The analysis of enantiomers of the total hydrolysate showed that the peptidoglycan type of strain M3^T was L-Lys–D-Asp (type A4α), characteristic of all *Lysinibacillus* species (Ahmed et al. 2007). Whole-cell sugar analysis revealed the presence of ribose and glucose.

The major polar lipids in strain M3^T were diphosphatidylglycerol (DPG), phosphatidylethanolamine (PE), phosphatidylglycerol (PG), and two unknown phospholipids (Fig. S5). The cellular fatty acid profile contained high proportions of iso-$C_{15:0}$, $C_{16:1}\omega7c$ alcohol, and iso-$C_{16:0}$. The chemotaxonomic characteristics of strain M3^T are consistent with those expected of the genus (Ahmed et al. 2007). However, considerable differences in the proportions of the major menaquinones and fatty acids, and the composition of polar lipids were observed. These differences indicate the divergence of strain M3^T from its closest relatives.

Secondary metabolite biosynthetic gene clusters in strain M3^T

The biosynthetic potential of strain M3^T was assessed using antiSMASH v7.0 (Blin et al. 2023). This web server enables the identification, annotation, and analysis of gene clusters related to secondary metabolite production in bacterial genomes. Eight (8) secondary metabolite-producing BGCs belonging to different classes were predicted (Table 3). The number is comparable to those of *L. xylanilyticus* DSM 23,493^T and "*L. agricola*" FJAT-51,161^T, for which antiSMASH predicted 9 and 7 BGCs, respectively (Table S4).

BGCs involving PKS and PKS/NRPS hybrids

Non-ribosomal peptide synthetase (NRPS) and polyketide synthase (PKS) BGCs can produce a variety of antibiotics, anticancer agents, and immunosuppressants (Chen et al. 2019). In these clusters, synthesis is carried out by large modular enzymes. The structural and catalytic similarities between polyketides and non-ribosomal peptides allow for hybrid clusters that include components from both classes to introduce structural modifications in the major classes of BGCs and increase secondary metabolite variety (Mizuno et al. 2013; Belknap et al. 2020).

A type III PKS BGC and a hybrid PKS/NPRS BGC were identified by antiSMASH in the genome of strain M3^T. The 41-kb type III PKS BGC in region 5.1 comprises 46 genes. Comparisons within the MIBiG database (Terlouw et al. 2023) showed that the BGC was most similar to an alkylresorcinol BGC in *Streptomyces griseus* subsp. griseus NBRC 13,350, a type III PKS in *Candidatus entotheonella serta*, and hierridin B and C BGCs in *Cyanobium* sp. LEGE 06113 (Fig. S6). Alkylresorcinols have bioactivities that include antimicrobial, anticancer, lipid-lowering, and antioxidant properties (Zabolotneva et al. 2022).

A 71-kb PKS/NRPS cluster in region 13.1 was identified, comprising 37 putative ORFs consisting of biosynthesis, regulatory, and transporter genes (Fig. 5A and B). The cluster contained one type I PKS (*ABNX05_16725*), three NRPSs

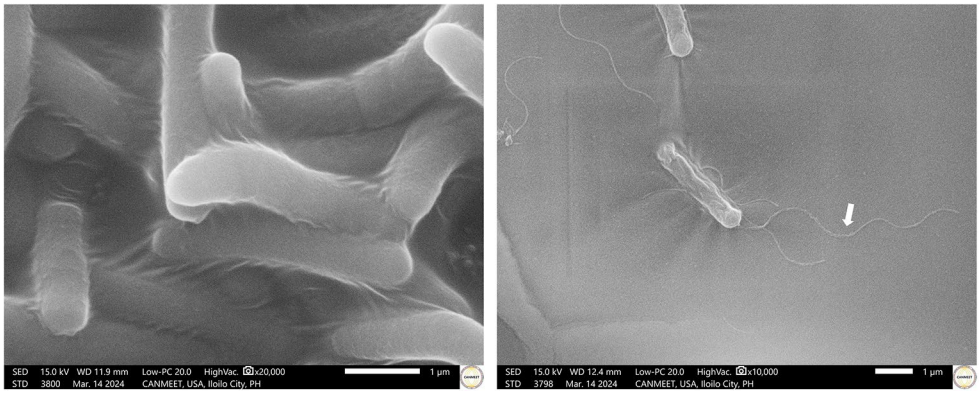

Fig. 4 Scanning electron micrographs of strain M3^T using JCM-7000 NeoScope™ Benchtop scanning electron microscope (Tokyo, Japan). (**A**) Strain M3^T cells have a rod-shaped morphology. (**B**) The white arrow shows a single flagella-like structure

Table 2 Chemotaxonomic characteristics of strain M3^T and closely related species

Chemotaxonomic characteristic	1	2 [a]	3 [a]	4 [a]	5 [b]
Major menaquinones (%)					
MK-5	-	NA	6.3	NA	NA
MK-6	5.8	NA	29.1	NA	13
MK-7	94.2	NA	58.3	NA	87
MK-8	-	NA	6.3	NA	NA
Major fatty acids (%)					
iso-$C_{14:0}$	3.0	1.6	4.7	2.6	1.7
$C_{14:0}$	0.5	0.9	0.6	0.4	0.4
iso-$C_{15:1}\omega10c$	1.1	NA	NA	NA	NA
iso-$C_{15:0}$	41.6	58.2	46.7	45.9	31.8
anteiso-$C_{15:0}$	1.6	8.0	6.9	7.4	21.4
$C_{15:0}$	1.0	0	0	0	0.5
$C_{16:1}\omega7c$	20.9	7.0	14.0	10.1	7.6
iso-$C_{16:0}$	19.0	1.8	15.8	12.2	11.2
$C_{16:1}\omega11c$	2.3	2.7	2.3	5.3	2.7
$C_{16:0}$	1.1	1.9	1.9	2.7	1.8
iso-$C_{17:1}\omega10c$	2.2	6.3	0.6	2.0	1.3
iso-$C_{17:1}\omega5c$	0.4	NA	NA	NA	NA
iso-$C_{17:0}$	4.3	3.4	3.3	6.1	5.5
anteiso-$C_{17:0}$	0.5	2.7	1.8	3.1	11.1
iso-$C_{18:0}$	0.1	NA	NA	NA	NA
Major polar lipids	DPG, PE, PG, and two unknown phospholipids	DPG, PE, PG	DPG, PE, one unknown aminolipid, two unknown aminophospholipids, two unknown phospholipids	DPG, PE, PG	DPG, PG

1, Strain M3^T; 2, *L. xylanilyticus* DSM 23,493^T; 3, "*L. agricola*" FJAT-51,161^T; 4, *L. macroides* DSM 54^T; 5, *L. boronitolerans* T-10a^T. All data was from this study unless indicated otherwise. -, no detected value; NA, no data available

[a]Data from Lu and Liu (2021), [b] Data from Ahmed et al. (2007)

DPG, diphosphatidylglycerol; PE, phosphatidylethanolamine; PG, phosphatidylglycerol

(*ABNX05_16700*, *ABNX05_16705*, and *ABNX05_16710*), a thioesterase (*ABNX05_16675*), an oxidoreductase (*ABNX05_16725*), and a 4′-phosphopantetheinyl transferase (PPT; *ABNX05_16670*). Gene *ABNX05_16675* was predicted to encode a 4′-PPT, a member of a family of enzymes involved in the synthesis of a wide range of compounds, such as fatty acid, polyketide, and non-ribosomal peptide metabolites (Copp and Neilan 2006; Beld et al. 2014). ClusterBlast revealed BGCs with low gene sequence similarities (31% being the highest) to those found within region 13.1 in different bacteria, including those belonging to the genera *Bacillus*, *Paenibacillus*, *Tumebacillus*, *Aquimarina*, *Myxococcus*, and *Kurthia* (Fig. S7). However, no similar gene clusters were identified using the KnownClusterBlast feature of antiSMASH. MIBiG comparison revealed that the PKS gene (*ABNX05_16725*) module had a 0.69 similarity score with the *cryB* gene of the hybrid NRPS/PKS cylindrospermospin BGC in *Aphanizomenon* sp. strains 10E9 and 22D11. The *ABNX05_16700*, *ABNX05_16705* and *ABNX05_16710* NRPS modules shared some similarity with NRPS genes involved in the biosynthesis of compounds with varying biological activities (Fig. S8). The observed MIBiG similarities result from the general organization and domains present in NRPS, PKS, and hybrid NRPS/PKS BGCs.

BGCs involving RiPPs

Ribosomally synthesized and post-translationally modified peptides (RiPPs) exhibit great structural and functional diversity (Zhong et al. 2020). Lanthipeptides, for example, are a class of RiPPs that prevent cell wall biosynthesis and disrupt cell membrane integrity (Li et al. 2021). A RiPP BGC encodes one or more precursor peptides and post-translational maturation enzymes. The maturation enzymes introduce modifications to the core peptide before proteolytic release from the leader peptide, increasing structural diversity (Repka et al. 2017; Mordhorst et al. 2023).

Table 3 List of putative secondary metabolite-producing biosynthetic clusters as predicted by antiSMASH

S/*N*	Region	Type	From	To	Most similar known cluster	% Similarity
1	2.1	NRPS-independent siderophore	150,898	164,459	Petrobactin	33
2	2.2	Terpene	506,205	527,026		
3	5.1	T3PKS	59,197	100,279	Bacillibactin/bacillibactin E and F (NRP)	30
4	5.2	Lanthipeptide class II	118,248	145,823	Gramicidin S (NRP)	6
5	7.1	RiPP-like	175,172	187,106	NA	NA
6	13.1	NRPS, T1PKS	14,770	85,865	NA	NA
7	15.1	Opine-like metallophore	25,102	47,240	Bacillopaline (Metallophore)	25
8	33.1	Betalactone	12,482	36,136	Fengycin (NRP)	46

NA, not reported by antiSMASH

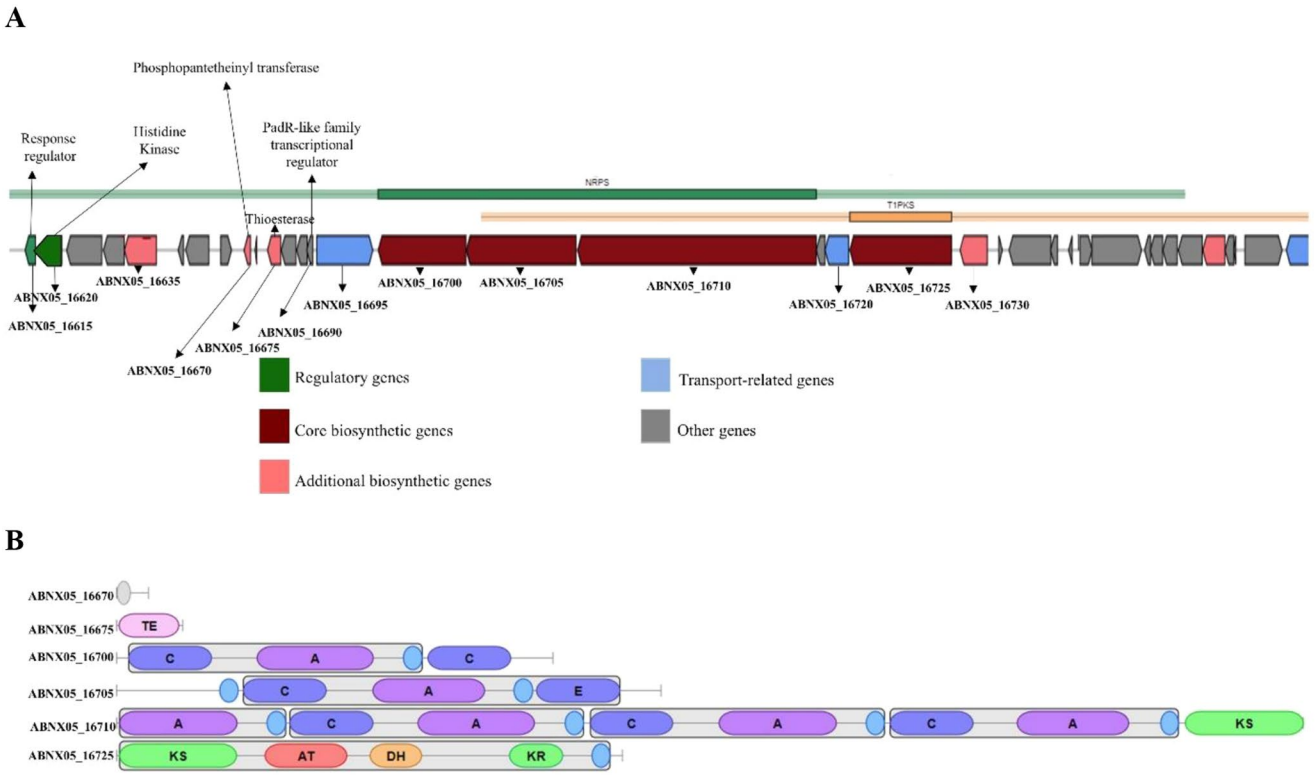

Fig. 5 Genetic organization of the hybrid PKS/NRPS BGC in region 13.1 of strain M3^T. (**A**) Genetic organization of the cluster, as annotated by antiSMASH. (**B**) Domain organization of the PKS and NRPS genes and the downstream thioesterase (TE) domain. The type I PKS consists of a ketosynthase (KS), an acyltransferase (AT), a dehydratase (DH), a ketoreductase, and an acyl carrier protein (ACP) domain. The NPRSs consist of condensation (**C**), adenylation (**A**), peptidyl carrier protein (PCP), epimerization (**E**), and ketosynthase (KS) domains

BAGEL analysis (van Heel et al. 2018) revealed three RiPPs (Table S5). Contig_20.12 and Contig_3.4 were predicted to contain RiPP-like BGCs; however, certain core genes, including core peptides, were not predicted (Fig. S9). Of particular interest was Contig_5.42.AO1_01 (region 5.2 in antiSMASH), which was predicted to encode a class II lanthipeptide (Table S5 and Fig. 6). In class II lanthipeptides, a single bi-functional enzyme, LanM, catalyzes the dehydration and cyclization processes of a precursor peptide(s). LanM contains an N-terminal dehydratase domain with minimal sequence similarity to other known enzymes, and the C-terminal cyclization domain shares significant sequence similarity with class I LanC cyclases (Blin et al. 2014). Following modification, LanT, an ABC transporter with an ATP-binding domain, cleaves a leader peptide at a highly conserved double glycine motif associated with the export of the mature peptides outside of the cell (Nishie et al. 2009, 2011). The predicted class II lanthipeptide BGC identified in the genome of strain M3^T included 4 predicted core peptides (*ABNX05_09170*, *ABNX05_09175*, *ABNX05_09180*, and *ABNX05_09185*), 2 modification enzymes (*ABNX05_09165* and *ABNX05_09190*), 1 transport and leader cleavage gene (*ABNX05_09160*), 2 immunity/transport genes (*ABNX05_09130* and *ABNX05_09200*), and 4 regulatory genes (*ABNX05_09135*, *ABNX05_09140*,

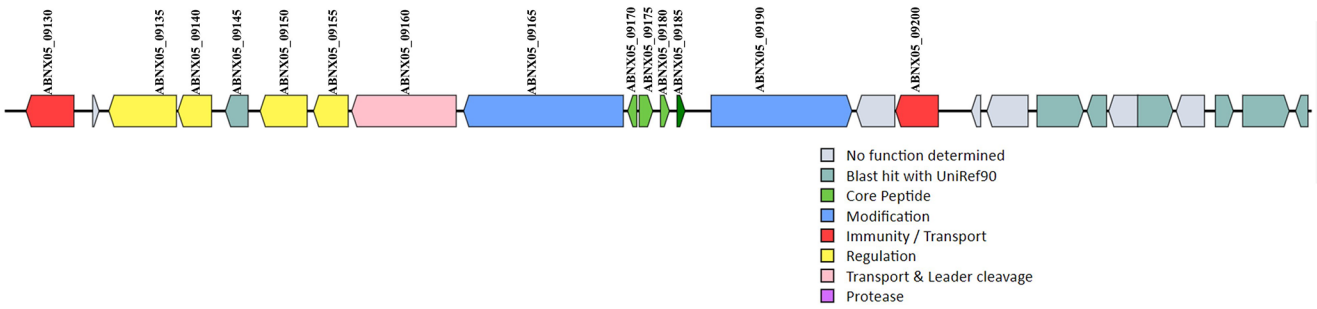

Fig. 6 Genetic organization of the lanthipeptide II BGC in strain M3^T, as predicted by BAGEL4

ABNX05_09150, and *ABNX05_09155*); it appears complete (Fig. 6).

Using RiPPMiner (Agrawal et al. 2017), we found that core peptide genes (*ABNX05_09170* to *ABNX05_09185*) shared a sequence similarity ranging from 35.42 to 46.67% with the core peptides of some class II bioactive lanthipeptides including haloduracin α (*Bacillus halodurans* C-125), geobacillin II (*Geobacillus thermodenitrificans* NG80-2, and lichenicidin VK21A2 (*Bacillus licheniformis*).

Other BGCs in strain M3^T

Terpenes and terpenoids exhibit an array of biological activities including antimicrobial, antitumor, anti-inflammatory, and antioxidant activities (Masyita et al. 2022). A terpene BGC was identified in region 2.2. In the MIBiG database, the core biosynthetic gene, a predicted squalene/phytoene synthase, shared the highest similarity score (0.32) with the core biosynthetic gene involved in the biosynthesis of squalestatin S1 by *Aspergillus* sp. Z5 (Fig. S10A). Squalestatins are a class of potent squalene synthase inhibitors mostly found in various fungal taxa (Lebe and Cox 2019).

The predicted betalactone BGC in region 33.1 had the highest similarity to a gene in a saccharide BGC involved in the production of mid-chain acyl sugars in the genome of the plant *Solanum lycopersicum* (Fig. S10B). The BGC had many biosynthetic enzymes that may be involved in other pathways in strain M3^T.

Region 2.1 was predicted to encode an NRPS-independent siderophore BGC involved in the biosynthesis of petrobactin, a siderophore produced by *Bacillus anthracis* Ames, according to MIBiG comparisons (Fig. S11A). Siderophores increase the uptake of iron (Ahmed and Holmström 2014). Their applications include enhancing the growth of unculturable microorganisms and promoting the growth and yield of plants; some have been shown to possess antimalarial and anticancer properties (Saha et al. 2016).

The opine-like metallophore BGC in region 15.1 has a low similarity score with the bacillopaline BGC in *Paenibacillus mucilaginosus* KNP414 (Fig. S11B). Opine metallophores are produced by two core enzymes: a nicotianamine synthase and an opine dehydrogenase, both detected in strain M3^T. Although their functions have not been well-established, they were found to be associated with virulence in *Staphylococcus aureus* and *Pseudomonas aeruginosa* (McFarlane and Lamb 2017).

In summary, strain M3^T is a novel species based on 16 S rRNA gene sequence similarity, dDDH and ANI values, phenotypic characterization, and chemotaxonomic analyses. Strain M3^T contains putative BGCs similar to active ones found in other organisms but differing in DNA sequence. Owing to the low similarity scores and support from related studies, the secondary metabolite BGCs of the isolate require further investigation.

Description of *Lysinibacillus zambalensis* sp. nov.

Lysinibacillus zambalensis (zam.ba.len'sis. N.L. masc. adj. *zambalensis*, pertaining to Zambales, where the type strain was isolated).

Aerobic, Gram-stain-positive, non-motile, rod-shaped bacterium. On TSB plate, colonies are round, creamy white, with an entire margin, raised elevation, and opaque. The cell size is approximately 3 µm in length and 0.6 µm in width. Growth occurs at 25–37 °C (optimal 30 °C), and a pH range of 6–10 (optimal 8), and 0.5–3% (w/v) NaCl (optimal 0.5%). The cells form ellipsoidal terminal endospores. Catalase positive, citrate negative, indole negative, lysine decarboxylase positive, methyl red negative, nitrate reduction negative, oxidase negative, urease negative, and Voges-Proskauer negative. Exhibits sensitivity to ciprofloxacin and penicillin G. The result from the BIOLOG GEN III assay indicates the utilization of acetic acid, acetoacetic acid, D-fructose-6-PO_4, D-gentibiose, D-lactic acid methyl ester, D-turanose, formic acid, glycerol, inosine, L-alanine, L-aspartic acid, L-fucose, L-glutamic acid, L-lactic acid, N-acetyl-D-glucosamine, N-acetyl-β-D-mannosamine, propionic acid, tween 40, α-hydroxy-butyric acid, β-hydroxy-D, L-butyric acid, and α-keto-butyric acid. Results indicate partial utilization of D-fucose, D-fructose, D-galactose, D-glucose-6-PO_4, D-melibiose, dextrin, β-methyl-D-glucoside, glucuronamide, gelatin, L-malic

acid, N-acetyl-D-galactosamine, and N-acetyl neuraminic acid. Showed tolerance to 1% sodium lactate, guanidine HCl, lithium chloride, potassium tellurite, sodium bromate, and sodium butyrate. Negative results are recorded for 3-methyl glucose, α-D-Glucose, D-maltose, α-D-lactose, α-keto-glutaric acid, bromo-succinic acid, citric acid, D-arabitol, D-aspartic acid, D-cellobiose, D-galacturonic acid, D-gluconic acid, D-glucuronic acid, D-mannose, D-mannitol, D-malic acid, D-raffinose, D-salicin, D-serine, D-sorbitol, D-saccharic acid, D-trehalose, γ-amino-butyric acid, glycyl-L-proline, L-arginine, L-histidine, L-pyroglutamic acid, L-rhamnose, L-serine, L-galactonic acid lactone, methyl pyruvate, mucic acid, myo-inositol, p-hydroxy-phenylacetic acid, pectin, quinic acid, stachyose, and sucrose. Negative results for the chemical sensitivity tests include 8% NaCl, fusidic acid, tetrazolium blue, and tetrazolium violet. The major respiratory quinone is MK-7 and the major polar lipids are diphosphatidylglycerol (DPG), phosphatidylethanolamine (PE), phosphatidylglycerol (PG), and two unknown phospholipids. The predominant cellular fatty acid is iso-$C_{15:0}$ and the peptidoglycan type is L-Lys–D-Asp (type A4α). The G+C content of the genome is 36.5%.

The type strain, designated M3^T (=TISTR 10640^T=BIOTECH 10973^T), is isolated from water collected from the Poon Bato hyperalkaline spring in Zambales province, Philippines. The GenBank accession numbers for the 16 S rRNA gene and the genome of the type strain are PQ061501 and JBEGDG000000000, respectively.

Supplementary Information The online version contains supplementary material available at https://doi.org/10.1007/s00203-025-04316-0.

Acknowledgements We would like to acknowledge Gamaliel Cabria (University of Waikato), Vina Argayosa, Camille Flores, and Rosalyn Diaz (Microbiological Research and Services Laboratory, Natural Sciences Research Institute, University of the Philippines Diliman) for their invaluable help in the microbiology portion of the work. We gratefully acknowledge the University of San Agustin, Center for Advanced New Materials, Engineering, and Emerging Technologies (CANMEET) in Iloilo City for their invaluable assistance in SEM data acquisition and analysis.

Author contributions Author Contributions: Conceptualization: J.A.A., K.R.Q.L., J.E.H.L., D.S.D., R.L.D.; Methodology, J.A.A, L.D.L. K.R.Q.L., J.E.H.L., J.J.T.; Validation: J.A.A, L.D.L., J.E.H.L., E.J.S.; Formal analysis: J.A.A; Investigation: J.A.A., K.R.Q.L., J.J.T., E.J.S., C.A.A.; Resources: J.E.H.L. and D.S.D.; Data curation: J.A.A., L.D.L., J.J.T., J.E.H.L.; Writing—original draft preparation: J.A.A; Writing—review and editing: All authors; Supervision: J.E.H.L., D.S.D., R.L.D., C.A.A.; Funding acquisition: J.E.H.L. All authors have read and agreed to the published version of the manuscript.

Funding This research was funded by the in-house funds of the National Institute of Molecular Biology and Biotechnology, College of Science, University of the Philippines Diliman.

Data availability Strain M3^T was isolated from the Poon Bato Spring, Botolan, Zambales, Philippines. The isolate has been deposited in the Philippine National Collection of Microorganisms (UP Los Banos, Laguna, Philippines) under the accession number BIOTECH 10973^T, and in the Thailand Institute of Scientific and Technological Research (TISTR) Culture Collection (Pathum Thani, Thailand) under the accession number TISTR 10640^T. The draft genome sequence of strain M3^T has been deposited in the GenBank database under the accession number JBEGDG000000000. The GenBank accession number of the 16 S rRNA gene sequence of strain M3^T is PQ061501.

Declarations

Competing interests The authors declare no competing interests.

References

Agrawal P, Khater S, Gupta M, Sain N, Mohanty D (2017) RiPPMiner: a bioinformatics resource for deciphering chemical structures of RiPPs based on prediction of cleavage and cross-links. Nucleic Acids Res 45:W80–W88. https://doi.org/10.1093/nar/gkx408

Ahmad V, Khan MS (2015) Therapeutic intervention and molecular characterization of bacteriocin producing *Lysinibacillus* sp. nov. isolated from food sample. Pak J Pharm Sci 28:1337–1344

Ahmad V, Navalgund MZI, Haseeb M, Khan MS (2014) Antimicrobial potential of bacteriocin producing *Lysinibacillus* jx416856 against foodborne bacterial and fungal pathogens, isolated form fruits and vegetable waste. Anaerobe 27:87–95. https://doi.org/10.1016/j.anaerobe.2014.04.001

Ahmed E, Holmström SJ (2014) Siderophores in environmental research: roles and applications. Microb Biotechnol 7:196–208. https://doi.org/10.1111/1751-7915.12117

Ahmed I, Yakota A, Yamazoe A, Fujiwara T (2007) Proposal of *Lysinibacillus boronitolerans* gen. nov. sp. nov., and transfer of *Bacillus fusiformis* to *Lysinibacillus fusiformis* comb. nov. and *Bacillus sphaericus* to *Lysinibacillus sphaericus* comb. nov. Int J Sys Evol Microbiol 57:1117–1125. https://doi.org/10.1099/ijs.0.63867-0

Akahoshi DT, Bevins CL (2022) Flagella at the host-microbe interface: key functions intersect with redundant responses. Front Immunol 13:828758. https://doi.org/10.3389/fimmu.2022.828758

Alam K, Zhao Y, Lu X, Gong K, Zhong L, Hao J, Islam M, Islam S, Li G, Zhang Y, Li R, Li A (2022) Isolation, complete genome sequencing, and in silico genome mining of *Burkholderia* for secondary metabolites. BMC Microbiol 22:323. https://doi.org/10.1186/s12866-022-02692-x

Albarano L, Esposito R, Ruocoo N, Constantini M (2020) Genome mining as new challenge in natural products discovery. Mar Drugs 18:199. https://doi.org/10.3390/md18040199

Altschul SF, Madden TL, Schaffer AA, Zhang J, Zhang Z, Miller W, Lipman DJ (1997) Gapped BLAST and PSI-BLAST: A new generation of protein database search programs. Nucleic Acids Res 25:3389–3402. https://doi.org/10.1093/nar/25.17.3389

Amaresan N, Kumar MS, Annapurna K, Kumar K, Sankaranarayanan A (2020) Firmicutes. In: Beneficial Microbes in Agro-ecology. Acad Press, pp. 861–912. https://doi.org/10.1016/B978-0-12-823414-3.00018-6

Andrade A, Girón JA, Amhaz JMK, Trabulsi LR, Martinez MB (2002) Expression and characterization of flagella in nonmotile enteroinvasive *Escherichia coli* isolated from diarrhea cases. Infect Immun 70(10):5882–5886. https://doi.org/10.1128/IAI.70.10.5882-5886.2002

Aziz RK, Bartels D, Best AA et al (2008) The RAST server: rapid annotations using subsystems technology. BMC Genomics 9:75. https://doi.org/10.1186/1471-2164-9-75

Baculi RQ, Collado CI, Evangelista AD (2017) Molecular profile of alkaline enzyme-producing bacteria from serpentinization-driven spring in Zambales, Philippines. Asian Jr Microbiol Biotech Env Sci 19:204–215

Bankevich A, Nurk S, Antipov D, Gurevich AA, Dvorkin M, Kulikov AS, Lesin VM, Nikolenko SI, Pham S, Prjibelski AD, Pyshkin AV, Sirotkin AV, Vyahhi N, Tesler G, Alekseyev MA, Pevzner PA (2012) SPAdes: a new genome assembly algorithm and its applications to single-cell sequencing. J Comput Biol 19(5):455–477. https://doi.org/10.1089/cmb.2012.0021

Beld J, Sonnenschein EC, Vickery CR, Noel JP, Burkart MD (2014) The phosphopantetheinyl transferases: catalysis of a posttranslational modification crucial for life. Nat Prod Rep 31:61–108. https://doi.org/10.1039/c3np70054b

Belknap KC, Park CJ, Barth BM, Andam CP (2020) Genome mining of biosynthetic and chemotherapeutic gene clusters in *Streptomyces* bacteria. Sci Rep 10:2003. https://doi.org/10.1038/s41598-020-58904-9

Blackwood KS, He C, Gunton J, Turenne CY, Wolfe J, Kabani AM (2000) Evaluation of RecA sequences for identification of *Mycobacterium* species. J Clin Microbiol 38(8):2846–2852. https://doi.org/10.1128/jcm.38.8.2846-2852.2000

Bligh EG, Dyer WJ (1959) A rapid method of total lipid extraction and purification. Can J Biochem Physiol 37:911–917. https://doi.org/10.1139/o59-099

Blin K, Kazempour D, Wohlleben W, Weber T (2014) Improved lanthipeptide detection and prediction for antiSMASH. PLoS ONE 9:e103665. https://doi.org/10.1371/journal.pone.0089420

Blin K, Shaw SK, Augustijn HE, Reitz ZL, Biermann F, Alanjary M, Fetter A, Terlouw BR, Metcalf WW, Helfrich EJN, van Wezel GP, Medema MH, Weber T (2023) AntiSMASH 7.0: new and improved predictions for detection, regulation, chemical structures and visualisation. Nucleic Acids Res 51:W46–W50. https://doi.org/10.1093/nar/gkad344

Brettin T, Davis JJ, Disz T et al (2015) RASTtk: A modular and extensible implementation of the RAST algorithm for Building custom annotation pipelines and annotating batches of genomes. Sci Rep 5:8365. https://doi.org/10.1038/srep08365

Brink B (2010) Urease test protocol. ASM. https://asm.org/getattachment/ac4fe214-106d-407c-b6c6-e3bb49ac6ffb/urease-test-protocol-3223.pdf

Buxton R (2011) Nitrate and nitrite reduction test protocols. ASM. https://asm.org/ASM/media/Protocol-Images/Nitrate-and-Nitrite-Reduction-Test-Protocols.pdf?ext=.pdf

Cardace D, Meyer-Dombard DR, Woycheese KM, Arcilla CA (2015) Feasible metabolisms in high pH springs of the Philippines. Front Microbiol 6:10. https://doi.org/10.3389/fmicb.2015.00010

Chaban B, Hughes HV, Beeby M (2015) The flagellum in bacterial pathogens: for motility and a whole lot more. Semin Cell Dev Biol 46:91–103. https://doi.org/10.1016/j.semcdb.2015.10.032

Chalita M, Kim YO, Park S, Oh HS, Cho JH, Moon J, Baek N, Moon C, Lee K, Yang J, Nam GG, Jung Y, Na SI, Bailey MJ, Chun J (2024) EzBioCloud: a genome-driven database and platform for Microbiome identification and discovery. Int J Sys Evol Microbiol 74(6):006421. https://doi.org/10.1099/ijsem.0.006421

Chen R, Wong HL, Burns BP (2019) New approaches to detect biosynthetic gene clusters in the environment. Med (Basel) 6:32. https://doi.org/10.3390/medicines6010032

Chu J, Vila-Farres X, Inoyama D, Ternei M, Cohen LJ, Gordon EA, Reddy BVB, Charlop-Powers Z, Zebroski HA, Gallardo-Macias R, Jaskowski M, Satish S, Park S, Perlin DS, Freundlich JS, Brady SF (2016) Discovery of MRSA active antibiotics using primary sequence from the human Microbiome. Nat Chem Biol 12:1004–1006. https://doi.org/10.1038/nchembio.2207

Coorevits A, Dinsdale AE, Heyrman J, Schumann P, Van Landschoot AV, Logan NA, De Vos P (2012) *Lysinibacillus macroides* sp. nov., nom. rev. Int J Syst Evol Microbiol 62:1121–1127. https://doi.org/10.1099/ijs.0.027995-0

Copp JN, Neilan BA (2006) The phosphopantetheinyl transferase superfamily: phylogenetic analysis and functional implications in cyanobacteria. Appl Environ Microbiol 72:2298–2305. https://doi.org/10.1128/AEM.72.4.2298-2305.2006

Dicks LMT, Dreyer L, Smith C, van Staden AD (2018) A review: the fate of bacteriocins in the human gastro-intestinal tract: do they cross the gut-blood carrier. Front Microbiol 9:2297. https://doi.org/10.3389/fmicb.2018.02297

El-Sayed SE, Abdelaziz NA, Osman HH, El-Housseiny GS, Aleissawy AE, Aboshanab KM (2022) *Lysinibacillus* isolate MK212927: A natural producer of allylamine antifungal. 'terbinafine ' Molecules 27:201. https://doi.org/10.3390/molecules27010201

Felsenstein J (1981) Evolutionary trees from DNA sequences: a maximum likelihood approach. J Mol Evol 17(6):368–376. https://doi.org/10.1007/BF01734359

Felsenstein J (1985) Confidence limits on phylogenies: an approach using the bootstrap. Evolution 39(4):783–789. https://doi.org/10.1111/j.1558-5646.1985.tb00420.x

Fitch WM (1971) Toward defining the course of evolution: minimum change for a specific tree topology. Syst Zool 20(4):406–416. https://doi.org/10.1093/sysbio/20.4.406

Froböse NJ, Bjedov S, Schuler F, Kahl BC, Kampmeier S, Schaumburg F (2020) Gram staining: a comparison of two automated systems and manual staining. J Clin Microbiol 58(12):e01914–e01920. https://doi.org/10.1128/JCM.01914-20

Gokdemir FS, Aras S (2019) Chemotaxonomy in bacterial systematics. Commun Fac Sci Univ Ank Ser C 28:78–90

Goris J, Konstantinidis KT, Klappenbach JA, Coenye T, Vandamme P, Tiedje JM (2007) DNA-DNA hybridization values and their relationship to whole-genome sequence similarities. Int J Syst Evol Microbiol 57:81–91. https://doi.org/10.1099/ijs.0.64483-0

Huang X, Madan A (1999) CAP3: A DNA sequence assembly program. Genome Res 9(9):868–877. https://doi.org/10.1101/gr.9.9.868

Jamal QMS, Ahmad V (2022) *Lysinibacilli*: a biological factories intended for bio-insecticidal, bio-control, and bioremediation activities. J Fungi 8:1288. https://doi.org/10.3390/jof8121288

Kalkreuter E, Pan G, Cepeda AJ, Shen B (2020) Targeting bacterial genomes for natural product discovery. Trends Pharmacol Sci 41:13–26. https://doi.org/10.1016/j.tips.2019.11.002

Karthick P, Mohanraju R (2020) Antimicrobial compounds produced by *Lysinibacillus odysseyi* epiphytic bacteria associated with red algae. Braz J Microbiol 51:1683–1690. https://doi.org/10.1007/s42770-020-00341-x

Komaki H (2023) Recent progress of reclassification of the genus *Streptomyces*. Microorganisms 11(4):831. https://doi.org/10.3390/microorganisms11040831

Kong D, Wang Y, Zhao B, Li Y, Song J, Zhai Y, Zhang C, Want H, Chen X, Zhao B, Ruan Z (2014) *Lysinibacillus haloterans* sp. nov., isolated from saline-alkaline soil. Int J Syst Evol Microbiol 64:2593–2598. https://doi.org/10.1099/ijs.0.061465-0

Lal A, Cheeptham N (2015) Decarboxylase broth protocol. ASM. https://asm.org/ASM/media/Protocol-Images/Decarboxylase-Broth-Protocol.pdf?ext=.pdf

Lebe KE, Cox RJ (2019) Oxidative steps during the biosynthesis of squalestatin S1. Chem Sci 10:1227–1231. https://doi.org/10.1039/c8sc02615g

Lee CS, Jung Y, Park S, Oh T, Yoon J (2010) *Lysinibacillus xylanilyticus* sp. nov., a xylan-degrading bacterium isolated from forest humus. Int J Syst Evol Microbiol 60(2):281–286. https://doi.org/10.1099/ijs.0.013367-0

Lee I, Kim YO, Park S, Chun J (2016) OrthoANI: an improved algorithm and software for calculating average nucleotide identity. Int J Syst Evol Microbiol 66:1100–1103. https://doi.org/10.1099/ijsem.0.000760

Lee I, Chalita M, Ha SM, Na SI, Yoon S, Chun J (2017) ContEst16S: an algorithm that identifies contaminated prokaryotic genomes using 16S RNA gene sequences. Int J Syst Evol Microbiol 67:2053–2057. https://doi.org/10.1099/ijsem.0.001872

Lefort V, Desper R, Gascuel O (2015) FastME 2.0: A comprehensive, accurate, and fast distance-based phylogeny inference program. Mol Biol Evol 32:2798–2800. https://doi.org/10.1093/molbev/msv150

Li C, Alam K, Zhao Y, Hao J, Yang Q, Zhang Y, Li R, Li A (2021) Mining and biosynthesis of bioactive lanthipeptides from microorganisms. Front Bioeng Biotechnol 9:692466. https://doi.org/10.3389/fbioe.2021.692466

Lu J, Liu G (2021) *Lysinibacillus agricola* sp. nov., isolated from soil. Arch Microbiol 203:4173–4178. https://doi.org/10.1007/s00203-021-02394-4

MacWilliams MP (2009a) Citrate test protocol. ASM. https://asm.org/ASM/media/Protocol-Images/Citrate-Test-Protocol.pdf?ext=.pdf

MacWilliams MP (2009b) Indole test protocol. ASM. https://asm.org/getattachment/200d3f34-c75e-4072-a7e6-df912c792f62/indole-test-protocol-3202.pdf

Maela MP, van der Walt H, Serepa-Dlamini MH (2022) The antibacterial, antitumor activities, and bioactive constituents' identification of *Alectra sessiliflora* bacterial endophytes. Front Microbiol 13:870821. https://doi.org/10.3389/fmicb.2022.870821

Manni M, Berkeley MR, Seppey M, Simão FA, Zdobnov EM (2021) BUSCO update: novel and streamlined workflows along with broader and deeper phylogenetic coverage for scoring of eukaryotic, prokaryotic, and viral genomes. Mol Bio Evol 38:4647–4654. https://doi.org/10.1093/molbev/msab199

Masyita A, Sari RM, Astuti AD, Yasir B, Rumata NR, Emran TB, Nainu F, Simal-Gandara J (2022) Terpenes and terpenoids as main bioactive compounds of essential oils, their roles in human health and potential application as natural food preservatives. Food Chem X 13:100217. https://doi.org/10.1016/j.fochx.2022.100217

McDevitt S (2009) Methyl red and Voges-Proskauer test protocols. ASM. https://asm.org/getmedia/40946f85-9357-4563-aa8a-994427efa825/Methyl-Red-and-Voges-Proskauer-Test-Protocols.pdf

McFarlane JS, Lamb AL (2017) Biosynthesis of an opine metallophore by *Pseudomonas aeruginosa*. Biochemistry 56:5967–5971. https://doi.org/10.1021/acs.biochem.7b00804

Meier-Kolthoff JP, Göker M (2019) TYGS is an automated high-throughput platform for state-of-the-art genome-based taxonomy. Nat Commun 10:2182. https://doi.org/10.1038/s41467-019-10210-3

Meier-Kolthoff JP, Carbasse JS, Peinado-Olarte RL, Göker M (2022) TYGS and LPSN: A database tandem for fast and reliable genome-based classification and nomenclature of prokaryotes. Nucleic Acids Res 50:801–D807. https://doi.org/10.1093/nar/gkab902

Mizuno CM, Kimes KE, Lopez-Perez M, Auso E, Rodriguez-Valera F, Ghai R (2013) A hybrid NRPS-PKS gene cluster related to the bleomycin family of antitumor antibiotics in *Altromonas macleodii* strains. PLoS ONE 8:e76021. https://doi.org/10.1371/journal.pone.0076021

Monciardini P, Iorio M, Maffioli S, Sosio M, Donadio S (2014) Discovering new bioactive molecules from microbial sources. Microb Biotechnol 7:209–220. https://doi.org/10.1111/1751-7915.12123

Monnin C, Quéméneur M, Price R, Jeanpert J, Maurizot P, Boulart C, Donval J, Pelletier B (2021) The chemistry of hyperalkaline springs in serpentinizing environments: 1. The composition of free gases in new Caledonia compared to other springs worldwide. J Geophys Res Biogeo 126:e2021JG006243. https://doi.org/10.1029/2021JG006243

Mordhorst S, Ruijne F, Vagstad AL, Kuipers OP, Piel J (2023) Emulating nonribosomal peptides with ribosomal biosynthetic strategies. RSC Chem Biol 4:7–36. https://doi.org/10.1039/D2CB00169A

Mounyr B, Moulay S, Saad KI (2016) Methods for *in vitro* evaluating antimicrobial activity: a review. J Pharm Anal 6(2):71–79. https://doi.org/10.1016/j.jpha.2015.11.005

Na SI, Kim YO, Yoon SH, Sung-min H, Baek I, Chun J (2018) UBCG: Up-to-date bacterial core gene set and pipeline for phylogenomic tree reconstruction. J Microbiol 56(4):280–285. https://doi.org/10.1007/s12275-018-8014-6

Nam Y, Seo M, Lim S, Lee S (2012) Genome sequence of *Lysinibacillus boronitolerans* F1182, isolated from a traditional Korean fermented soybean product. J Bacteriol 194:5988. https://doi.org/10.1128/JB.01485-12

Naureen Z, Rehman NU, Hussain H, Hussain J, Gilani S, Al Housni SK, Mabood F, Khan AL, Farooq S, Abbas G, Harrasi AA (2017) Exploring the potentials of *Lysinibacillus sphaericus* ZA9 for plant growth promotion and biocontrol activities against phytopathogenic fungi. Front Microbiol 8:1477. https://doi.org/10.3389/fmicb.2017.01477

Ngalimat MS, Rahman RNZ, Yusof MT, Syahir A, Sabri S (2019) Characterisation of bacteria isolated from stingless bee, *Heterotrigona itama*, honey, bee bread and propolis. PeerJ 7:e7478. https://doi.org/10.7717/peerj.7478

Nishie M, Shioya K, Nagao J, Jikuya H, Sonomoto K (2009) ATP-dependent leader peptide cleavage by NukT, a bifunctional ABC transporter, during lantibiotic biosynthesis. J Biosci Bioeng 108:460–464. https://doi.org/10.1016/j.jbiosc.2009.06.002

Nishie M, Sasaki M, Nagao J, Zendo T, Nakayama J, Sonomoto K (2011) Lantibiotic transporter requires cooperative functioning of the peptidase domain and the ATP binding domain. J Biol Chem 286:11163–11169. https://doi.org/10.1074/jbc.M110.212704

Olson RD, Assaf R, Brettin T et al (2023) Introducing the bacterial and viral bioinformatics resource center (BV-BRC): A resource combining PATRIC, IRD, and vipr. Nucleic Acids Res 51:D678–689. https://doi.org/10.1093/nar/gkac1003

Ouoba LI, Mbozo ABV, Thorsen L, Anyogu A, Nelson DS, Kobawila SC, Sutherland JP (2015) *Lysinibacillus Louembei* sp. nov., a spore-forming bacterium isolated from Ntoba Mbodi, alkaline fermented leaves of cassava from the Republic of Congo. Int J Syst Evol Microbiol 65:4256–4262. https://doi.org/10.1099/ijsem.0.000570

Overbeek R, Olson R, Pusch GD et al (2014) The SEED and the rapid annotation of microbial genomes using subsystems technology (RAST). Nucleic Acids Res 42:D206–D214. https://doi.org/10.1093/nar/gkt1226

Parks DH, Imelfort M, Skennerton CT, Hugenholtz P, Tyson GW (2015) CheckM: assessing the quality of microbial genomes recovered from isolates, single cells, and metagenomes. Genome Res 25(7):1043–1055. https://doi.org/10.1101/gr.186072.114

Parte AC (2013) LPSN–list of prokaryotic names with standing in nomenclature. Nucleic Acids Res 42(Database issue):D613–D616. https://doi.org/10.1093/nar/gkt1111

Pradhan AK, Pradhan N, Sukla LB, Panda PK, Mishra BK (2014) Inhibition of pathogenic bacterial biofilm by surfactant produced by *Lysinibacillus fusiformis* S9. Bioprocess Biosyst Eng 37:139–149. https://doi.org/10.1007/s00449-013-0976-5

Reiner K (2010) Catalase test protocol. ASM. https://asm.org/getattachment/72a871fc-ba92-4128-a194-6f1bab5c3ab7/Catalase-Test-Protocol.pdf

Repka LM, Chekan JR, Nair SK, van der Donk WA (2017) Mechanistic understanding of lanthipeptide biosynthetic enzymes. Chem Rev 117:5457–5520. https://doi.org/10.1021/acs.chemrev.6b00591

Saha M, Sarkar S, Sarkar B, Sharma BK, Bhattacharjee S, Tribedi P (2016) Microbial siderophores and their potential applications: A review. Environ Sci Pollut Res Int 23:3984–3999. https://doi.org/10.1007/s11356-015-4294-0

Saitou N, Nei M (1987) The neighbor-joining method: a new method for reconstructing phylogenetic trees. Mol Biol Evol 4(4):406–425. https://doi.org/10.1093/oxfordjournals.molbev.a040454

Schaeffer AB, Fulton MD (1933) A simplified method of staining endospores. Science 77(1990):194. https://doi.org/10.1126/science.77.1990.194

Scherlach K, Hertweck C (2021) Mining and unearthing hidden biosynthetic potential. Nat Commun 12:3864. https://doi.org/10.1038/s41467-021-24133-5

Schumann P (2011) Peptidoglycan structure. Methods Microbiol 38:101–129. https://doi.org/10.1016/B978-0-12-387730-7.00005-X

Senthilraj R, Prasad GS, Janakiraman K (2016) Sequence-based identification of microbial contaminants in non-parenteral products. Braz J Pharm Sci 52(2):329–336. https://doi.org/10.1590/S1984-82502016000200011

Shields P, Cathcart L (2010) Oxidase test protocol. ASM. https://asm.org/getattachment/00ce8639-8e76-4acb-8591-0f7b22a347c6/oxidase-test-protocol-3229.pdf

Stackebrandt E, Goebel BM (1994) Taxonomic note: A place for DNA-DNA reassociation and 16S rRNA sequence analysis in the present species definition in bacteriology. Int J Syst Evol Microbiol 44(4):846–849. https://doi.org/10.1099/00207713-44-4-846

Sun J, Xu L, Wu X (2017) *Lysinibacillus alkalisoli* sp. nov.; isolated from saline-alkaline soil. Int J Syst Evol Microbiol 67:67–71. https://doi.org/10.1099/ijsem.0.001571

Tambekar DH, Tambekar SD, Rajgire AV, Jadhav AS, Sawale KK (2016) Isolation and characterization of amylase from *Lysinibacillus xylanilyticus* from alkaline environment. Int J Res Stud Biosci 4:21–24. https://doi.org/10.20431/2349-0365.0406001

Tamura K, Stecher G, Kumar S (2021) MEGA11: molecular evolutionary genetics analysis version 11. Mol Biol Evol 38:3022–3027. https://doi.org/10.1093/molbev/msab120

Tang X, Li J, Millán-Aguiñaga N, Zhang JJ, O'Neill EC, Ugalde JA, Jensen PR, Mantovani SM, Moore BS (2015) Identification of thiotetronic acid antibiotic biosynthetic pathways by target-directed genome mining. ACS Chem Biol 10:2841–2849. https://doi.org/10.1021/acschembio.5b00658

Tang Y, Lei J, Ma X, Li J, Li H, Liu Z (2023) Identification and characterization of a novel bacteriocin cluster in *Lysinibacillus boronitolerans*. Biotechnol Appl Biochem 70:1860–1869. https://doi.org/10.1002/bab.2488

Terlouw BR, Blin K, Navarro-Muñoz JC et al (2023) MIBiG 3:0: A community-driven effort to annotate experimentally validated biosynthetic gene clusters. Nucleic Acids Res 51:D603–D610. https://doi.org/10.1093/nar/gkac1049

Thompson JD, Higgins DG, Gibson TJ (1994) CLUSTAL W: improving the sensitivity of progressive multiple sequence alignment through sequence weighting, position-specific gap penalties and weight matrix choice. Nucleic Acids Res 22(22):4673–4680. https://doi.org/10.1093/nar/22.22.4673

Umehara Y, Aoyagi H (2023) Development of simple cultured cell-anaerobic microbial co-culture system using liquid paraffin. J Bioscience Eng 135(6):487–492. https://doi.org/10.1016/j.jbiosc.2023.03.008

van Heel AJ, de Jong A, Song S, Viel JH, Kok J, Kuipers OP (2018) BAGEL4: A user-friendly web server to thoroughly mine RiPPs and bacteriocins. Nucleic Acids Res 46:W278–W281. https://doi.org/10.1093/nar/gky383

Vieira S, Huber KJ, Neumann-Schaal M, Geppert A, Luckner M, Wanner G, Overmann J (2021) *Usitatibacter rugosus* gen. nov., sp. nov. and *Usitatibacter palustris* sp. nov., nov el members of *Usitatibacteraceae* fam. nov. within the order *Nitrosomonadales* isolated from soil. Int J Syst Evol Microbiol 71:004631. https://doi.org/10.1099/ijsem.0.004631

Wang L, Lee F, Tai C, Kasai H (2007) Comparison of the *GyrB* gene sequences, 16S rRNA gene sequences and DNA-DNA hybridization in the *Bacillus subtilis* group. Int J Syst Evol Microbiol 57(8):1846–1850. https://doi.org/10.1099/ijs.0.64685-0

Wang J, Fan Y, Yao Z (2010) Isolation of a *Lysinibacillus fusiformis* strain with teterodoxin-producing ability from puffer fish *Fugu obscurus* and the characterization of this strain. Toxicon 56:640–643. https://doi.org/10.1016/j.toxicon.2010.05.011

Yang S, Lin C, Sung CT, Fang J (2014) Antibacterial activities of bacteriocins: application in foods and pharmaceuticals. Front Microbiol 5:241. https://doi.org/10.3389/fmicb.2014.00241

Yu L, Tang X, Wei S, Qiu Y, Xu X, Xu G, Wang Q, Yang Q (2019) Isolation and characterization of a novel piezotolerant bacterium *Lysinibacillus yapensis* sp. nov., from deep-sea sediment of the Yap Trench, Pacific Ocean. J Microbiol 57(7):562–568. https://doi.org/10.1007/s12275-019-8709-3

Zabolotneva AA, Shatova OP, Sadova AA, Shestopalov AV, Roumiantsev SA (2022) An overview of alkylresorcinols biological properties and effects. J Nutr Metab 2022:4667607. https://doi.org/10.1155/2022/4667607

Zhang L, Xu Z, Patel BKC (2007) *Bacillus decisifrondis* sp. nov., isolated from soil underlying decaying leaf foliage. Int J Syst Evol Microbiol 57(Pt 5):974–978. https://doi.org/10.1099/ijs.0.64440-0

Zhong Z, He B, Li J, Li Y (2020) Challenges and advances in genome mining of ribosomally synthesized and post-translationally modified peptides (RiPPs). Synth Sys Biotechnol 5:155–172. https://doi.org/10.1016/j.synbio.2020.10.001